Engineered Water Repellency for Frost Mitigation: Practical Modeling Considerations

John L. Daniels, P.E., F.ASCE[1]; William G. Langley, Ph.D., P.E.[2];
Michael Uduebor[3]; and Bora Cetin, Ph.D., M.ASCE[4]

[1]Professor and Chair, Dept. of Civil and Environmental Engineering, Univ. of North Carolina at Charlotte, Charlotte, NC. Email: jodaniel@uncc.edu
[2]Research Professor, Dept. of Civil and Environmental Engineering, Univ. of North Carolina at Charlotte, Charlotte, NC. Email: wlangley@uncc.edu
[3]Ph.D. Student, Dept. of Civil and Environmental Engineering, Univ. of North Carolina at Charlotte, Charlotte, NC. Email: muduebor@uncc.edu
[4]Associate Professor, Dept. of Civil and Environmental Engineering, Michigan State Univ., East Lansing, MI. Email: cetinbor@msu.edu

ABSTRACT

Engineered water repellency has the potential to mitigate frost heave in geotechnical systems such as roads and foundations. Models can be used to inform design approaches and predict performance; the literature is replete with general models of frost action. There are comparatively fewer reports on how to practically incorporate the effect of mineral surfaces, pore fluid composition, and engineered water repellency into thermo-hydro-mechanical-chemical (THMC) models. An aspect of such models involves describing the state of pore fluid in the frozen fringe and unfrozen soil beneath an impinging freezing front and growing ice lens. Capillary and osmotic gradients are created as ice formation reduces moisture content while increasing the concentration of ions in the remaining unfrozen pore fluid. The work reported here is part of a larger effort to quantify the relative role of osmotic and matric potential on frost heaving, while exploring the use of organosilanes to mitigate ice lens formation and growth. As a precursor to incorporating the broader array of physicochemical processes in frost action, this paper reviews the sensitivity of unsaturated flow to changes in contact angle. Unsaturated flow gradients are created in response to simulated matric, osmotic, and cryogenic suction within a two-dimensional model. Results indicate that an increased contact angle results in a reduction in unsaturated flow, regardless of induced gradient.

INTRODUCTION

Few soil processes involve as many physico-chemical phenomena as frost action. Frost susceptible soils are typically of intermediate hydraulic conductivity (e.g., silty soils that display high capillary rise within a relatively short period of time) whereby significant volumes of water can be drawn by suction to the freezing front, forming segregated layers of ice lenses. Ice lenses can be very large, on the order of millimeters to centimeters to as much as meter-scale. This behavior has long been recognized, with Taber (1916, 1929, 1930) documenting continuous vertical displacement via successive ice lens formation and growth. Many states limit the fines content in roadway base course material to less than 12%, as studies have shown that frost heave increases linearly with increasing fines (e.g., Hatipoglu et al. (2020), Haider et al. (2016), Konrad and Lemieux (2005), Tester and Gaskin (1996)).

As ice forms in the pore space of saturated soil, it generates positive pore water pressure in the adjacent unfrozen water. Effective stresses approach zero until eventually soil particles are separated by a distinct lens of ice. Beneath this lens (toward the "warm" side), desaturation of the pore space results in capillary suction and a hydraulic gradient from warmer, unfrozen locations to the ice lens. And as pore water freezes, ions are mostly excluded and further concentrated in the remaining unfrozen water. The highest concentrations are found immediately in front of the freezing front, with solute concentrations at the freezing front estimated to be 80 times the original pore fluid concentration (Kay and Groenevelt 1983). These ions increase the osmotic suction and the cumulative hydraulic gradient toward the freezing front. Together, these osmotic and capillary components represent the cryogenic suction effects that are a function of the phase change from water to ice. Other processes remain in effect, including capillary suction present in variably-saturated, unfrozen pore space, osmotic suction according to the prevailing unfrozen pore fluid composition in bulk and adsorbed water, and adsorption attributed to electrostatic, and van der Waals forces.

We can describe the state of moisture in terms of a change in total chemical potential (Δu_t), relative to "free" water in a reference condition. This allows us to explicitly identify known mechanisms, namely cryogenic capillary potential (Δu_{cc}), cryogenic osmotic potential (Δu_{co}), matric potential (Δu_m), which includes capillary (Δu_c), electrostatic (Δu_e) and van der Waals (Δu_v) potentials, as well as osmotic potential (Δu_o). Adapting from Lu and Likos (2004):

Δu_t = cryogenically induced change in potential + prevailing unfrozen change in potential

$$\Delta u_t = (\Delta u_{cc} + \Delta u_{co}) + (\Delta u_m + \Delta u_o) = (\Delta u_{cc} + \Delta u_{co}) + (\Delta u_c + \Delta u_e + \Delta u_v) + \Delta u_o \quad (1)$$

Each of these components influences the extent to which water can travel from a source to a growing ice lens, thereby contributing to heave. When predicting frost heave, the combined effect of cryogenically-induced and prevailing osmotic and matric forces has given rise to apparent contradictions and inaccuracies (Marion 1995). Yet existing literature and models do not quantify the role and relative significance of osmotic and matric forces in frost susceptible soils. One objective of this paper is to conceptually and numerically model the significance of these various components on the rate and extent of water migration. Another objective is to explore the extent to which all these components can be mitigated through the creation of a water repellent layer. In practice, this involves spraying an exposed layer with the organo-silane solution and allowing it to dry or using the solution as the molding moisture content during compaction control (Keatts et al. 2018). Injection and infiltration techniques can also deliver organo-silanes for post-construction or remediation applications. For modeling, this involves specification of a governing contact angle to reflect the extent of water repellency.

MATERIALS AND METHODS

A numerical model was created in COMSOL Multiphysics, v. 5.5. The model is set up as a 2D vertical column (6 cm diameter, 24 cm height) with an axis of symmetry about z axis. Two soil types were modeled, using properties given by Rawls et al. (1982) for "silty clay loam" and "silty clay", both of which represent soil types that are frost susceptible. The model was used to model a basic "capillary" experiment under transient conditions to consider water saturation, pressure, and temperature. The intent was to conceptually evaluate the effect of increased suction that develops in response to frost action. At any given point in time, the combined effects of all changes in potential can be incorporated into Terzaghi's (1943) theory for capillary rise:

$$i = (h_c - z)/z \quad (2)$$

In the Eq. (2), i represents the hydraulic gradient, z is the height at any point in time and h_c is the height of capillary rise. Values h_c were estimated following an equation presented by Kumar and Malik (1990), as shown with other soil properties in Table 1. Model fluid properties are shown in Table 2.

Table 1. Soil properties used in modeling effort.

Property	Silty Clay	Silty Clay Loam
Saturated hydraulic conductivity, cm/s	2.50×10^{-5}	4.17×10^{-5}
Air entry pressure, kPa	28.6	30.1
Porosity	0.42	0.43
Pore size distribution index	0.127	0.151
Contact Angle - Untreated	0	0
Contact Angle – Water Repellent Layer, degrees	80	80
Height of capillary rise, cm	157	156

Table 2. Fluid Properties used in modeling effort

Property	Water	Air
Density	1000 kg/m³	1 kg/m³
Dynamic Viscosity	0.001 Pa·s	1.76E-5 Pa·s

As such, the capillary gradient was larger than the model height, ensuring that an initially unsaturated domain would be subject to capillary rise. This reflects a field condition in which a frost susceptible soil is close to the water table. The model solves for air saturation, water flow, and water pressure due to capillary forces as well as heat transfer between lower boundary (liquid water at ambient temperature) and upper boundary (cold air at ground surface modeled as negative heat flux). The soil column is initially filled with air and water with an initial water saturation of 0.50. The Brooks and Corey (1964) model for capillary pressure and relative permeabilities is used for the time-dependent simulation. The boundary conditions for bottom and top boundaries for Darcy's law are the atmospheric pressure for water phase at the bottom and the hydrostatic atmospheric pressure minus the capillary pressure at the top. For the phase transport (air and water), there is no flux assumed for the air phase at the bottom boundary. At the top boundary, a mass flux for the air phase is defined which results from the pressure gradient given in the Darcy model. Zero fluxes for water and air are specified along the sides of the column.

The heat transfer component of the model solves for temperatures of four materials in the model domain: liquid water, ice, air and the soil matrix. It also predicts the change of phase liquid water to ice. (COMSOL 2019a). A single set of thermodynamic properties in Table 3 was used for both soil matrix types (COMSOL 2019b). The initial temperature for water, air, and soil matrix in the heat transfer model was 5 °C. The boundary conditions for bottom and top boundaries for heat transfer are water inflow at 5 °C at the bottom and heat extraction at the top (ground surface, see Results and Discussion). Along the sides of the column, zero flux for heat is specified. The water-to-ice phase change model parameters are: phase change temperature -0.5 °C, temperature transition interval 20 °C, and latent heat for phase change 334 kJ/kg (COMSOL 2019b).

Table 3. Thermodynamic Properties used in modeling effort

Material Property	Ice	Water	Soil Matrix
Density	920 kg/m3	1000 kg/m3	2650 kg/m3
Heat capacity at constant pressure	2060 J/(kg·K)	4182 J(kg·K)	835 J(kg·K)
Thermal conductivity	2.14 W/(m·K)	0.6 W/(m·K)	9 W/(m·K)

RESULTS AND DISCUSSION

Several scenarios were modeled: (1) initial capillary rise, (2) heat extraction initiated at top boundary, (3) increased suction, and (4) effect of water repellency. While both soils had similar predicted heights of capillary rise, the variation in reported air entry pressure and pore size distribution index results in different rates of capillary rise (Figure 1). When subjected to heat extraction at the surface (1 kW/m^2), frost action is initiated and a phase change occurs in both soils, as noted in Figure 2. Figure 2 shows that the rate of frost penetration of silty clay loam soil is higher than that of silty clay while the final frost depth of each soil after 1600 s is similar.

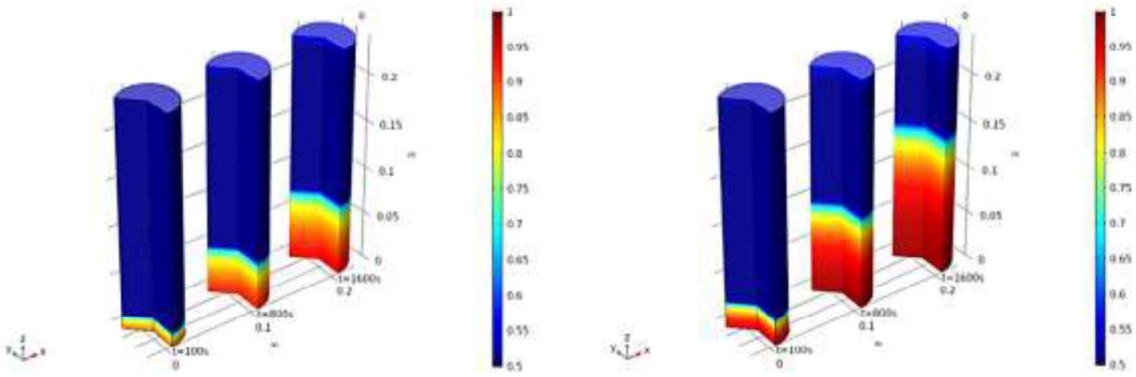

Figure 1. Capillary rise in 1600 seconds for silty clay (left) and silty clay loam (right). Dark red color represents increased degree of saturation. Blue color represents initial degree of saturation (0.50).

The effect of freezing on the hydraulic gradient induced by frost action can be conceptually modeled as an increase in suction. For conceptual purposes, an increase in 40 kPa was applied beneath the location of the ice lens, to simulate the effect of cryogenic capillary and cryogenic osmotic suction. Osmotic pressures that approach the magnitude of matric potential have been reported (e.g., Fredlund et al. 2012) and are especially likely to develop cryogenically. The effect of this increase was to draw an increasing amount of water toward the upper boundary and location of ice. Next model runs were performed by increasing the prevailing contact angle from 0 to 80. This increase in hydrophobicity simulates the effect of engineered water repellency and reduces the extent to which any change in moisture potential, cryogenic or otherwise, can induce water flux. Figure 3 presents a graph comparing the volumetric flux of water through the base of the column for all conditions (matric, increased suction, repellent) while Figure 4 show the effect of repellency on capillary rise.

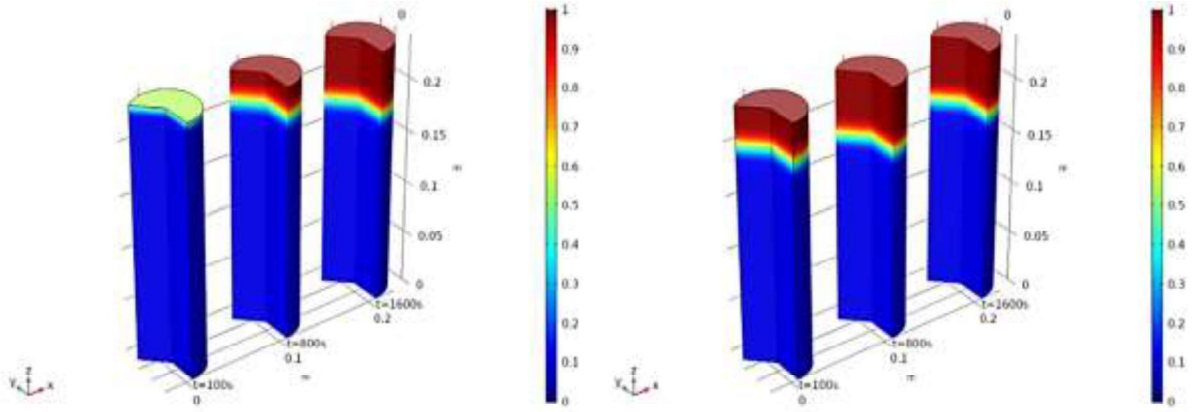

Figure 2. Frost penetration in 1600 seconds for silty clay (left) and silty clay loam (right), dark red color represents a phase change from water to ice. Blue color represents unfrozen water.

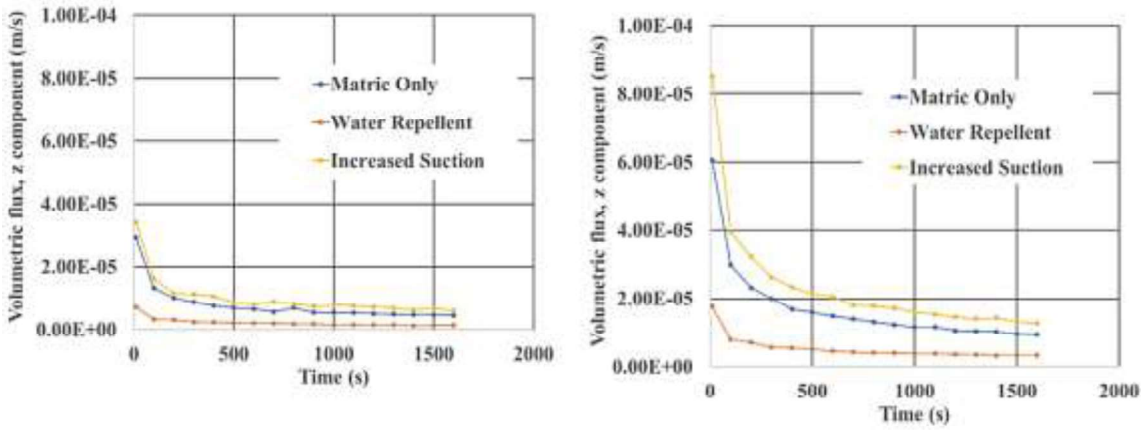

Figure 3. Effect of matric, increased suction and water repellency on volumetric flux (through base of column with access to water supply); silty clay (left), silty clay loam (right).

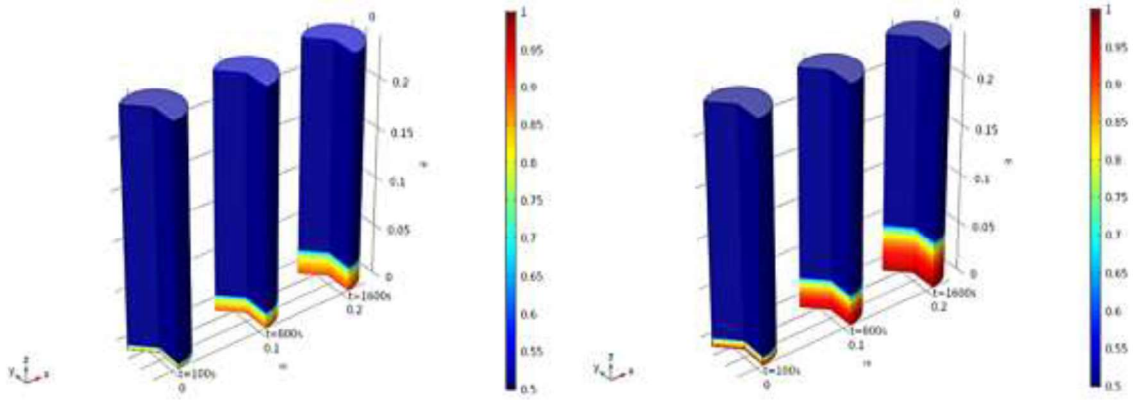

Figure 4. Capillary rise in 1600 seconds for silty clay (left) and silty clay loam (right), with engineered water repellency. Dark red color represents increased degree of saturation.

For engineered water repellency applications, a contact angle of greater than 90 is typically used, e.g., Mahedi et al. (2020), Daniels (2020). These larger values are especially important in applications where the goal is to mitigate water/frost infiltration under positive pressure, as in the case of covers for waste containment, or ponding above other geosystems such as foundations over expansive soils. However, in the case of frost mitigation, water flux occurs under tension, and less hydrophobicity is required to serve as a "capillary break". The modeling presented herein provides a conceptual approach for exploring the extent to which multiple components of moisture potential can affect volumetric flux. Additional work will involve explicitly coupling the process of ice lens formation with desaturation, along with changes in effective stress.

CONCLUSIONS

Frost action results in changes in moisture potential, which in turn create a hydraulic gradient. There are multiple components to this gradient however a conceptual modeling effort suggests that they can all be arrested using engineered water repellency. The modeling results show that soil type and hydrophobicity levels of the medium have an impact on frost action and needs to be studied further.

REFERENCES

Daniels, J. L. (2020) "Engineered Water Repellency for Applications in Environmental Geotechnology" In: Reddy, K. R., Agnihotri A. K., Yukselen-Aksoy Y., Dubey B. K., Bansal A. (eds) *Sustainable Environmental Geotechnics. Lecture Notes in Civil Engineering*, vol 89. Springer, Cham. https://doi.org/10.1007/978-3-030-51350-4_6.

Brooks, R. H., and Corey, A. T. (1964) "Hydraulic Properties of Porous Media", *Hydraulic Papers*, Colorado State University, March 1964, Fort Collins, CO.

COMSOL Multiphysics. (2019a) *Heat Transfer Module User's Guide*, pp. 469-481. COMSOL Multiphysics® v. 5.5. COMSOL AB, Stockholm, Sweden. 2019.

COMSOL Multiphysics. (2019b) *Frozen Inclusion, Table 1*. COMSOL Multiphysics® v. 5.5. COMSOL AB, Stockholm, Sweden. 2019.

Fredlund, D. G., Rahardjo, H., and Fredlund, M. D. (2012) *Unsaturated Soil Mechanics*, Wiley, New York, p. 112.

Haider, I., Kaya, Z., Cetin, A., Hatipoglu, M., Cetin, B., and Aydilek, A. H. (2014) "Drainage and Mechanical Behavior of Highway Base Materials," *Journal of Irrigation and Drainage Engineering ASCE*, vol. 140(6), article no. 04014012.

Hatipoglu, M., Cetin, B., and Aydilek, A. H. (2020) "Effects of Fines Content on Hydraulic and Mechanical Performance of Unbound Granular Base Aggregates," *Journal of Transportation Engineering, Part B: Pavements*, 146(1), article no. 04019036.

Kay, B. D., and Groenevelt, P. H. (1983) The redistribution of solutes in freezing soil: Exclusion of solutes. In *4th International Conference on Permafrost*, Jul 17-22, Fairbanks, Alaska, Washington, DC, National Academy Press, 584–588.

Keatts, M. I., Daniels, J. L., Langley, W. G., Pando, M. A., and Ogunro, V. O. (2018) "Apparent contact angle and water entry head measurements for organo-silane modified sand and coal fly ash", *ASCE Journal of Geotechnical and Geoenvironmental Engineering*, vol. 144(6), 1-9.

Konrad, J. M., and Lemieux, N. (2005) “Influence of fines on frost heave characteristics of a well graded base-course material”, *Canadian Geotechnical Journal*, vol. 42, 515–527.
Kumar, S., and Malik, R. S. (1990) “Verification of quick capillary rise approach for determining pore geometrical characteristics in soils of varying texture”, *Soil Science*, 150(6), 883-888.
Lu, N., and Likos, W. J. (2004) *Unsaturated soil mechanics*. John Wiley and Sons, Inc., Hoboken, NJ, 556 p.
Mahedi, M., Satvati, S., Cetin, B., and Daniels, J. L. (2020) “Chemically Induced Soil Water Repellency and the Freeze-Thaw Durability of Soils”, *ASCE Journal of Cold Regions Engineering*, 34(3) pp. 1-7.
Marion, G. M. (1995) Freeze-Thaw Processes and Soil Chemistry. Special Report, 95-12, U.S. Army Cold Regions Research and Engineering Laboratory, Hanover, NH.
Tester, R. E., and Gaskin, P. N. (1996) “Effect of fines content on frost heave”, *Canadian Geotechnical Journal*, vol. 33, 678–680.
Rawls, W. J., Brakensiek, D. L., and Saxton, K. E. (1982) “Estimation of Soil Water Properties”. *Transactions of the ASAE*, Vol. 25, No. 5, 1316-1320. American Society of Agriculture Engineers, St. Joseph, Michigan.
Taber, S. (1916) “The growth of crystals under external pressure”, *American Journal of Science*, 4th Series, vol. 246, 532–556.
Taber, S. (1929) “Frost heaving”, *Journal of Geology*, vol. 37(1), 428–461.
Taber, S. (1930) “The mechanics of frost heaving”, *Journal of Geology*, vol. 38(4), 303–317.
Terzaghi. (1943) *Theoretical Soil Mechanics*, Wiley, New York.